



Published in final edited form as:

Expert Opin Drug Deliv. 2014 December ; 11(12): 1913–1922. doi:10.1517/17425247.2014.941354.

Ferritins as Nanoplatforms for Imaging and Drug Delivery

Zipeng Zhen¹, Wei Tang¹, Trever Todd¹, and Jin Xie^{1,2,*}

¹Department of Chemistry, University of Georgia, Athens, Georgia 30602, United States

²Bio-Imaging Research Center (BIRC), University of Georgia, Athens, Georgia 30602, United States

Abstract

Introduction—Due to unique architecture and surface properties, ferritin has emerged as an important class of biomaterial. Many studies suggest that ferritin and its derivatives hold great potential in a wide range of bio-applications.

Areas covered—In this review, we summarize recent progress on employing ferritins as a platform to construct functional nanoparticles for applications in magnetic resonance imaging (MRI), optical imaging, cell tracking, and drug delivery.

Expert opinion—As a natural polymer, ferritins afford advantages such as high biocompatibility, good biodegradability, and a relatively long plasma half-life. These attributes put ferritins ahead of conventional materials in clinical translation for imaging and drug delivery purposes.

Keywords

Ferritin; nanomedicine; magnetic resonance imaging; drug delivery; reporter gene

1. Introduction

Nanoparticle-based drugs have emerged as an important category of therapeutics. A myriad of nanoparticles, such as metals, metal oxides, carbon nanotubes, liposomes, and polymers, have been investigated as drug delivery nanocarriers [1,2]. These nanocarriers exhibit a large surface area and sometimes a central cavity that allows them to load a high payload of therapeutics [3]. With proper surface modification, systematically injected nanocarriers can stay in the circulation for a relatively long period of time, and selectively accumulate at tumors where blood vessels are hyperpermeable and the lymphatic system is compromised [4]. Tumor targeting ligands can also be conjugated onto the surface of nanocarriers. The resulting conjugates can bind to a specific biomarker of tumors, a feature that can further enhance the tumor selectivity [5].

*Address correspondence to: Professor Jin Xie, Telephone number: (706) 522-1933, Fax number: (706) 542-9454, ; Email: jinxie@uga.edu

Financial and competing interests disclosure

This work was supported by an NCI/NIH R00 grant (R00CA153772), an Elsa U. Pardee foundation grant, and a UGA startup grant. The authors have no other relevant affiliations or financial involvement with any organization or entity with a financial interest in or financial conflict with the subject matter or materials discussed in the manuscript apart from those disclosed.

Despite the extensive and intensive efforts at the pre-clinical level, however, few nanoparticle-based drugs have been approved for clinical use. Major factors that impede the translation include toxicity and immunogenicity, as many of the currently used nanocarriers are made of exogenously synthesized materials or contain heavy-metals [6]. Due to this consideration, there has been a recent interest in research to develop protein-based carriers for drug delivery. Unlike polymers or metals, proteins often have minimal toxicity and immunogenicity, and can be easily degraded after the therapy has concluded [7]. These advantages put them ahead of conventional materials in clinical translation. One successful example is Abraxane, which is an albumin-bound paclitaxel nanoparticulate formulation. Abraxane has been approved by the FDA to treat breast cancer, non-small-cell lung cancer (NSCLC), and pancreatic cancer [8].

Along this line, many have investigated ferritin and its derivatives as a novel type of nanoplatform [9–12]. Ferritin is an iron storage and transport protein that is found in most living organisms including humans [13]. Artificially expressed ferritins afford a large central cavity, which, according to recent studies, can load transition metals or certain molecules with high efficiency [9,11]. The surface of ferritins can be easily modified via either chemical or genetic modifications to introduce functionalities [14,15]. All of these attributes suggest ferritin and its derivatives as a powerful system with potential uses for both imaging and drug delivery.

In this review we summarize recent progress on applications of ferritin and its derivatives for MRI, optical imaging, and drug delivery. We also include discussions on surface modification strategies for ferritins to obtain formulations suitable for different uses.

2. Architecture and surface properties of ferritins

Ferritin is a nearly ubiquitous protein found in animals, higher plants, and various microorganisms (fungi and bacteria) [13]. It has evolved to function as a primary iron transportation mechanism, and it also plays essential roles in iron storage and recycling. A large protein with a mass of 450 kDa, ferritin is composed of 24 subunits, including both heavy (H-chains, 21 kDa) and light (L-chains, 19 kDa) chains. They self-assemble to form a spherical, cage-like structure that has inner and outer dimensions of ~8 and ~12 nm, respectively (Figure 1a–c) [16]. The composition of ferritins, i.e. the H-chain to L-chain ratio, varies among ferritins from different tissues. For instance, for human ferritins, H-chain predominates in the heart, while L-chain is overexpressed in the liver [17]. Ferritins from different species share the cage-like structure and extensive homology in sequence [18]. For instance, there is 93% sequence similarity of H-chain between murine ferritins and ferritins from humans [19]. For artificial ferritins, many investigations, including ours, have focused on H-chain ferritin.

One ferritin protein can store up to ~4,500 iron atoms as mineral ferrihydrite [17, 20]. In addition to Fe, other metallic species, such as Cu [21], Co [22], and Gd [23] are also amenable to encapsulation by ferritins. Taking advantage of this property, several groups have reported synthesis of nanoparticles using ferritins as nanoreactors. For instance, Sun et al. successfully assembled gold nanostructures inside a ferritin cavity, and used the resulting

particles as optical probes for fluorescence imaging [11]. Okuda et al. reported synthesis of CeO₂ nanoparticles using ferritins as templates. The resulting nanoparticles can self-assemble to form three-dimensional arrays of CeO₂ nanoparticles with either an octahedral- or prism-like morphology [24].

There are both hydrophilic and hydrophobic channels (about 3–4 Å wide [25]) on the surface of ferritins, and these channels are believed to be the pathways for metallic cations, such as Fe(II), to pass in and out of the protein nanocages [13, 20]. Recent studies on hepatic ferritins showed that the mineral cores are composed of eight subunits, consistent with the eight channels in the protein shell that deliver iron to the central cavity [20]. It is believed that Fe cations are internalized through these channels and form ~ 2nm ferrihydrites around the interior channel entrances. A similar transportation mechanism may be responsible to the internalization of other species into the ferritins. These include molecules with diameters larger than Fe(II) (e.g. sucrose and ferrioxamine B [13]) or even the size of the channels [26]. These observations suggest the flexibility of the channels and the potential of ferritins as carriers for many species. Furthermore, despite the rigidity under physiological environments, ferritin nanocages can be broken down to subunits when the pH is lowered to 2~3 [27,28]. Interestingly, the process is reversible. When pH is tuned back to neutral, the 24 subunits can reassemble to constitute a nanocage, and almost in an intact fashion (Figure 1d). This pH-mediated nanocage assembly and disassembly further expand the nanosystem's capacity for loading. A number of molecules, such as Gd-HPDO3A (Gadoteridol) [29], methylene blue [30], cisplatin, and carboplatin [31] have been encapsulated into ferritins by employing this method.

The ability to disassemble and reassemble the nanocage also offers a unique and facile method to construct hybrid ferritin nanocages presenting multiple functionalities on the surface [15]. As an example, Lin et al. recently used this method to prepare hybrid ferritins presenting both Cy5.5, a near-infrared dye molecule, and RGD4C, a tumor targeting ligand with high binding affinity toward integrin $\alpha_v\beta_3$ [32], on the surface [9]. By adjusting the initial ratios between Cy5.5 and RGD4C presenting ferritins, the composition and the integrin binding affinity of the resulting hybrid ferritins can be tuned [10,15].

Ferritins can be easily modified to impart functionalities onto the surface. This can be achieved by coupling to the lysine and cysteine on the ferritin surface. For instance, dye molecules [15], quencher molecules [10], peptides [33], and antibody fragments [14] have been chemically conjugated onto the surface of ferritin with success. Moreover, motifs can be introduced onto the ferritin surface via genetic modification of the ferritin sequence [12,34].

3. Ferritins for MR imaging

Autologous ferritins have been investigated in vivo as a MRI indicator for several pathologies. For instance, MRI can estimate iron storage and tissue damage in patients with neurodegenerative disorders, such as Alzheimer's disease (AD) and Huntington's disease (HD) [35]. This is because these neurodegenerative disorders are often associated with

disrupted iron metabolism in the basal ganglia, and the resulting enhanced ferritin-bound Fe concentration can be detected as hypointensities on T2/T2*-weighted MR maps.

After surface engineering, ferritins can also be used as T2/T2* imaging probes. For instance, cationized ferritins have been used for kidney MRI. Briefly, ferritins were coupled with *N,N*-dimethyl-1,3 propanediamine (DMPA) by 1-ethyl-3-(3-dimethylaminopropyl) carbodiimide (EDC) activation of carboxyl groups [36] to become positively charged. When these cationic ferritins were systematically injected, they accumulated in the kidneys because the glomerular basement membrane is negatively charged [37–39]. This results in contrast enhancement that facilitates MR imaging of kidneys (Figure 2). It was found in rats that individual glomerulus can be visualized by gradient-echo MRI using these cationic ferritins as contrast agents. 3-D imaging can not only discern each glomerulus, but also the intrarenal distribution profile of glomerular volumes [39–41].

Ferritin can also be used as a MRI reporter gene to assist tracking of exogenously introduced cells. For instance, Campan et al. studied human ferritin H-chain as a reporter gene for in vivo tracking of stem cells by cardiac MRI [42]. They transduced swine cardiac stem/progenitor cells to overexpress ferritins and cultured the cells to obtain cardiospheres. When intramyocardially injected to rats with myocardial infarction, the cardiospheres homed to the infarction sites and the migration was successfully detected by T2*-weighted MRI. In another report, Cohen et al. transduced C6 cells with enhanced green fluorescent protein (EGFP) and influenza hemagglutinin (HA)-tagged ferritins using tetracycline (TET) as a transactivator gene [43]. The TET-regulated gene expression was able to be dynamically detected by MRI, and the result was validated by both fluorescence microscopy and histology assay. The same group later generated TET:EGFP-HA-ferritin (tet-hfer) transgenic mice [44]. With these mice, they showed that TET-regulated ferritin concentration in the liver and endothelial cells in the brain can be measured by T2 relaxometry with MRI. Overall, however, the relatively low sensitivity of ferritins has limited their uses as a tool for cell tracking.

In addition to taking up endogenous iron, ferritins can also be artificially loaded with magnetic species. For instance, Cao et al. added $(\text{NH}_4)_2\text{Fe}(\text{SO}_4)_2$ to a solution of H-chain ferritin with pH 8.5 at 65°C in an anaerobic chamber [45]. Under this condition, a single-crystal magnetite core with an average diameter of 5.2 ± 1.0 nm was generated within the nanocage. The resulting nanoparticles showed a transverse relaxivity r_2 (a measure of the ability of contrast agents to shorten T2 relaxation times) of $224 \text{ mM}^{-1}\text{s}^{-1}$, which is significantly higher than endogenous ferritins [46]. When injected into MDA-MB-231 tumor-bearing mice, a remarkable signal drop in tumors was observed on T2-weighted MR images. According to the authors, the tumor accumulation was attributed to interactions between ferritins and transferrin receptor 1 (TfR1) that is overexpressed on the surface of MDA-MB-231 cells [44,47]. Uchida et al. reported that the size of iron oxide nanoparticles produced by ferritins can be adjusted by controlling the Fe loading rates [34]. By increasing the loading from 1000 to 5000 Fe/ferritin, the core size was increased from 3.8 to 6.0 nm, and the magnetic properties were changed accordingly [34].

Ferritins can also serve as nanoreactors to produce other types of magnetic nanoparticles. Sanchez et al. reported that 5 nm Gd-nanoparticles can be produced within the ferritin cavity by adding $\text{Gd}(\text{NO}_3)_3 \cdot 6\text{H}_2\text{O}$ to apoferritin solutions [23]. The resulting particles displayed longitudinal and transverse relaxivities that were 10 and 70 times higher than clinically approved paramagnetic Gd-chelates, such as Gd-DTPA. Kalman et al. produced a manganese-based MRI contrast agent by partial reduction/dissolution of solid $\beta\text{-MnOOH}$ inside apoferritin cavities. The resulting conjugates contain up to 300–400 Mn(II) aqua ions in each apoferritin cavity, and a very high r_1 relaxivity of 4,000–7,000 s^{-1} per apoferritin unit was observed with these nanoparticles [48].

Ferritins can also encapsulate metal-chelates into the central cavity. As an example, Aime et al. employed pH-mediated nanocage disassembly and reassembly to load Gd-HPDO3A into the cavity of ferritins. According to the authors, an average of 8–10 Gd-HPDO3A molecules can be encapsulated into each apoferritin nanocage (Figure 3) [29]. The resulting Gd-loaded ferritin exhibited r_1 relaxivity of 80 $\text{mM}^{-1}\text{s}^{-1}$ on a per Gd basis, which is among the highest reported [29]. When coupled with C3d--a peptide specific for receptors on vessel endothelium, and intravenously (i.v.) injected to tumor endothelial cell (TEC) tumor bearing mice, signal increase in tumors by 30% was observed, indicating the potential of the formulation as a MRI contrast probe [49].

4. Ferritins for optical imaging

The surface of ferritins can be conjugated with dye molecules, and the resulting nanoparticles can be used as optical imaging probes. For instance, Lin et al. labeled ferritins with Cy5.5, a near-infrared dye molecule (ex/em: 675/695 nm), by reacting with primary amine groups on the ferritin surface [10]. These Cy5.5 conjugated ferritins were then mixed with genetically modified ferritins that presented RGD4C on the surface. By subjecting the mixture to pH-mediated nanocage disassembly and reassembly, Lin et al. obtained hybrid nanoparticles having both Cy5.5 and RGD on the surface. With the Cy5.5 as an optical tag, the distribution of the ferritins can be easily tracked in vitro and in vivo. When systematically injected to U87MG tumor bearing mice, these ferritins were found to be able to accumulate efficiently at tumors. RGD-integrin interactions were identified as the primary mechanism behind the tumor targeting, while the tumor enhanced permeability and retention (EPR) effect also had played a role in the process [10].

Ferritins can also be harnessed to construct protease activatable optical probes. Lin et al. reported a ferritin-based probe whose fluorescence is responsive to matrix metalloproteinases (MMPs) in the surroundings. Briefly, Cy5.5-Gly-*Pro-Leu-Gly-Val-Arg-Gly* and BHQ-3, separately, were conjugated onto two sets of ferritin nanocages [10]. *Pro-Leu-Gly-Val-Arg* (PLGVR) is a known substrate for multiple MMP members (e.g. MMP-2, -9, -13) [50,51]. BHQ-3 is a small molecule quencher of Cy5.5, which can (and only can) silence fluorescence of Cy5.5 when the two are in close vicinity (<10 nm). By mixing the two types of ferritin conjugates and subjecting them to pH-mediated hybridization, ferritin nanoparticles presenting both Cy5.5-GPLGVRG and BHQ-3 on the surface were yielded (Figure 4a). These ferritin conjugates are fluorescently silent at quiescent stage, but can be activated in an environment of high levels of MMPs, for instance in a tumor.

Recently, Sun et al. prepared H-chain ferritins encompassing two gold nanoclusters at the center of the ferritin cavity (Figure 4b) [11]. Due to strong binding of Au^{3+} to the imidazole ring, Au^{3+} can associate with the His residues at the ferroxidase center of H-ferritin (Figure 1c and 4b) [52,53], and be reduced to 1 nm gold nanoclusters in the presence of NaOH (1 M). Because each ferritin nanocage has multiple ferroxidase centers, two nanoclusters were formed in each nanocage. The observation concurs with the research by Pan et al. on cluster formation and growth in hepatic ferritins [20]. The nanocluster pair not only retains the intrinsic fluorescence of noble metals, but also gains enhanced and red-shifted emission due to the coupling interactions. In vitro studies with Caco-2 and HepG2 cells detected minimal cytotoxicity with these gold-loaded ferritins. The far-red fluorescence of the particles ensures good tissue penetration depth, allowing for the use of this nanosystem as a probe for in vivo imaging [11].

Given that there are multiple facile ways to modify ferritins, it is possible to incorporate more than one imaging feature into a single ferritin nanocage. For instance, Lin et al. successfully loaded ^{64}Cu , a radioisotope commonly used in positron emission tomography (PET), into ferritin nanocages that were surface-modified with RGD and Cy5.5. The resulting probes were proven to be effective for PET and fluorescence dually functional imaging [15]. Uchida et al. coupled fluorescein-5-maleimide onto the surface of iron-laden ferritins, and the obtained formulation, possessing both optical and magnetic properties, is a multifunctional nanoscale MR and fluorescence imaging probe with cell-specific targeting [34].

5. Ferritins for drug delivery

It is estimated that 30% of the worldwide population is iron deficient; most are women and children [54]. Ferritins have been intensively studied as an iron supplement for patients with the related diseases. Compared to their pure synthetic analogues, the 2–5 nm Fe(III) oxo-hydroxide core of ferritin is less ordered and thus more readily bioavailable. For instance, soybean seeds are used as a nonheme iron source because they contain a large amount of iron in the form of ferritin. It was found that women with marginal iron deficiency could metabolize 25.9 percent of soybean iron, a ratio that is much higher than other Fe sources, such as FeCl_3 [54,55]. On the other hand, it is challenging to use pure ferritin for iron supplementation given the required scale of purification and thus the overall costs. To address the issue, there have been recent efforts to prepare ferritin mimics with comparable bioavailability but lower costs. For instance, Powell et al. reported that tartrate can be used to co-precipitate with freshly formed ferrihydrite; the ligand markedly disrupts the ferrihydrite stability, mimicking the lability of ferritin cores [56]. Studies in murine models confirmed efficient absorption, suggesting the potential of the ferritin-core mimetic as cheap supplemental iron.

As mentioned above, in addition to Fe, other types of metals can be encapsulated into ferritins. These include radioactive isotopes, and the resulting ferritins can potentially be used for radiotherapy given the high loading efficiency and preferred pharmacokinetics of ferritins. In a previous study, Hainfeld et al. reported that ~ 800 ^{235}U atoms can be encapsulated into each ferritin nanocage [14]. Due to the high payload, the resulting

nanoparticles afford radiation sufficient to kill surrounding tumor cells. It is suggested that a similar strategy may be used to load and deliver other types of radioisotopes that have been used in the clinic such as ^{90}Y trium and ^{177}Lu tetium [57].

In addition to metals, some metal-containing small molecules can also be efficiently loaded into ferritins. Recently, Zhen et al. reported that doxorubicin (Dox)-Cu(II) complexes can be incorporated to RGD-modified ferritins (RFRTs) with high efficiency (73.49 wt %) (Figure 5a) [12]. As a comparison, individual Dox shows low loading efficiency, indicating an important role Cu(II) plays in the drug loading. With the ferritins as drug carriers, the circulation half-life of Dox was dramatically extended to 27 h, compared to that of 6.5 min for free Dox. When injected to U87MG tumor bearing mice, the Dox-loaded RFRTs (D-RFRTs) efficiently accumulated in tumors (Figure 5b) due to interactions between RGD and integrin $\alpha_v\beta_3$. Subsequent therapy studies showed that D-RFRTs can induce significantly improved tumor suppression efficiency compared to free Dox at the same dose. Meanwhile, cardiotoxicity, which is a primary side effect in Dox-based therapy, was significantly reduced when using ferritin as Dox carriers [12]. All of these studies suggest great potential of ferritin and its derivative as a novel type of Dox delivery vehicle.

More recently, Zhen et al. discovered that a metal-containing compound, ZnF_{16}Pc , can be encapsulated into RFRTs with an extremely high loading rate (up to 60 wt %) (Figure 5c) [9]. ZnF_{16}Pc has been studied as a photosensitizer for photodynamic therapy (PDT). Under photoirradiation by 671 nm light, ZnF_{16}Pc can transfer energy to near-by oxygen molecules to generate $^1\text{O}_2$, which is cytotoxic. Although ZnF_{16}Pc has poor water solubility, they can be well dispersed in aqueous solutions when loaded onto RFRTs. The resulting ZnF_{16}Pc -loaded RFRTs (P-RFRTs) showed selective phototoxicity to integrin $\alpha_v\beta_3$ positive cells. In vivo studies showed that P-RFRTs can efficiently home to tumors when systematically injected. With proper photoirradiation, the treatment caused efficient tumor growth arrest while not affecting surrounding normal tissues (Figure 5d). In particular, skin toxicity, a common side effect of PDT, was not observed with the treatment. This is attributable to ferritin-based delivery that results in minimal accumulation of ZnF_{16}Pc in the skin. It is postulated that the method can be extended to deliver other types of photosensitizers to facilitate their applications in tumor therapy.

6. Expert opinion

Despite the extensive promises, much work is needed before clinical translation of ferritins or their derivatives. For instance, despite the success of loading metals or molecules into the nanocages, the specific mechanisms of internalization into the cavity, and how and under what circumstances they are liberated are not fully known. Understanding the mechanisms will allow us to better engineer the protein nanocages for improved loading efficiency and controlled drug release. It is also possible, such as in the case of supplemental iron developments, to learn from the exploits such that ferritin mimics with comparable efficiency but lower costs can be obtained. On the other hand, more clinically related investigations are necessary to understand the fate of ferritin and its derivatives after systemic injection. This is especially important for ferritin-based therapeutics, where off-target damage is a critical criterion. One potential concern is the relatively high liver uptake

of ferritins. Previous studies showed that systematically injected ferritins can be cleared from the circulation and accumulated in organs such as the liver [58], largely due to the high expression of ferritin receptors in the organ [59]. It is thus worthwhile to explore the possibility of surface modification of ferritins (e.g. by PEGylation) to suppress the uptake and thereby extending the circulation. However, the modification may cause an adverse impact on the drug loading and integrity of the nanocages, which also needs thorough investigations.

While some researchers have suggested that ferritins can interact with transferrin receptor 1 that is expressed on the surface of many types of cancer cells [60,61], so far, most ferritin studies have utilized a targeting motif to achieve tumor targeting [62]. The targeting motifs can be imparted through genetic engineering, such as in the case of RGD modified ferritins. Whether or not such a change to the sequence may induce immunogenicity is largely unknown. It is also noted that currently, most basic research on ferritin-based imaging and therapy has been using murine ferritins. It is important in the future studies to engineer humanized ferritins and re-assess the performances.

As discussed above, ferritin as a nanoplatform can be used to construct imaging probes for optical, PET, or MR imaging. Among them, ferritin-based MRI probes are probably the most promising. Both T1 and T2 contrast agents of ferritin basis have been prepared and investigated. Both however, have their own sets of issues in terms of clinical translation. For T2-contrast probes, Fe-laden ferritin formulations of different forms have been prepared and investigated, many with heavier Fe loading than the wild-type ferritins. However, the relatively small cavity (and thus small particles that can be formed inside the protein cage) and the polycrystalline nature of the ferrihydrites make the magnetism of the mineral cores inferior to those formed by other synthetic approaches. For ferritin-based T1 imaging probes, Gd-loaded ferritins have been extensively studied and shown enhanced r1 relaxivity relative to the complex-based analogs [29]. One issue with Gd-based imaging probes, however, is the toxicity caused by free Gd [63]. Conventional Gd agents, due to relatively small sizes, are mostly excreted by renal clearance after systemic injection. For Gd-loaded ferritins, however, most Gd after injection may remain in the liver, and the subsequent metabolism and long-term impact is largely unknown.

Overall, ferritin and its derivatives are promising nanoplatforms. Compared with nanosystems made of artificial materials, ferritins hold a number of advantages including good biodegradability, low toxicity, long circulation half-lives, and facile surface modification. Different types of metals or small molecules have been successfully loaded into ferritins and the resulting conjugates have shown great perspectives in imaging and drug delivery. These features and advances suggest the great potential of ferritin formulations for clinical translation, but future investigations from both fundamental and clinical perspectives are needed.

Bibliography

Papers of special note have been highlighted as either of interest (•) or of considerable interest (••) to readers.

- 1••. Peer D, Karp JM, Hong S, et al. Nanocarriers as an emerging platform for cancer therapy. *Nat Nanotechnol.* 2007; 2:751–60. An important review summarizing the application of nano-sized carriers to cancer therapy. [PubMed: 18654426]
2. Hughes GA. Nanostructure-mediated drug delivery. *Nanomedicine.* 2005; 1:22–30. [PubMed: 17292054]
3. Ferrari M. Cancer nanotechnology: opportunities and challenges. *Nat Rev Cancer.* 2005; 5:161–71. [PubMed: 15738981]
4. Brannon-Peppas L, Blanchette JO. Nanoparticle and targeted systems for cancer therapy. *Adv Drug Deliv Rev.* 2004; 56:1649–59. [PubMed: 15350294]
- 5••. Jain RK, Stylianopoulos T. Delivering nanomedicine to solid tumors. *Nat Rev Clin Oncol.* 2010; 7:653–64. An important review summarizing the advantages of nanomedicine in fighting cancer. [PubMed: 20838415]
6. De Jong WH, Borm PJ. Drug delivery and nanoparticles: applications and hazards. *Int J Nanomedicine.* 2008; 3:133–49. [PubMed: 18686775]
7. Elzoghby AO, Samy WM, Elgindy NA. Protein-based nanocarriers as promising drug and gene delivery systems. *J Control Release.* 2012; 161:38–49. [PubMed: 22564368]
8. Green MR, Manikhas GM, Orlov S, et al. Abraxane, a novel Cremophor-free, albumin-bound particle form of paclitaxel for the treatment of advanced non-small-cell lung cancer. *Ann Oncol.* 2006; 17:1263–8. [PubMed: 16740598]
- 9•. Zhen Z, Tang W, Guo C, et al. Ferritin nanocages to encapsulate and deliver photosensitizers for efficient photodynamic therapy against cancer. *ACS Nano.* 2013; 7:6988–96. An important paper describing Zn-containing photosensitizer can be loaded into ferritin. [PubMed: 23829542]
- 10•. Lin X, Xie J, Zhu L, et al. Hybrid ferritin nanoparticles as activatable probes for tumor imaging. *Angew Chem Int Ed.* 2011; 50:1569–72. An excellent paper that describe the formulation of producing hybrid ferritin nanoparticles presenting functionalized probes on its surface.
- 11••. Sun CJ, Yang H, Yuan Y, et al. Controlling assembly of paired gold clusters within apoferritin nanoreactor for in vivo kidney targeting and biomedical imaging. *J Am Chem Soc.* 2011; 133:8617–24. An excellent paper describing “points of control” synthesis of two gold nanostructures inside of ferritin cavity. [PubMed: 21542609]
- 12•. Zhen Z, Tang W, Chen H, et al. RGD-modified apoferritin nanoparticles for efficient drug delivery to tumors. *ACS Nano.* 2013; 7:4830–7. An important paper describing Doxorubicin-Cu complex can be loaded into ferritin. [PubMed: 23718215]
- 13•. Munro HN, Linder MC. Ferritin: structure, biosynthesis, and role in iron metabolism. *Physiol Rev.* 1978; 58:317–96. An important review summarizing the ferritin’s structure and biosynthesis. [PubMed: 347470]
14. Hainfeld JF. Uranium-loaded apoferritin with antibodies attached - molecular design for uranium neutron-capture therapy. *Proc Natl Acad Sci USA.* 1992; 89:11064–8. [PubMed: 1438316]
15. Lin X, Xie J, Niu G, et al. Chimeric ferritin nanocages for multiple function loading and multimodal imaging. *Nano Lett.* 2011; 11:814–9. [PubMed: 21210706]
16. Marchetti A, Parker MS, Moccia LP, et al. Ferritin is used for iron storage in bloom-forming marine pennate diatoms. *Nature.* 2009; 457:467–70. [PubMed: 19037243]
- 17•. Theil EC. Ferritin: structure, gene regulation, and cellular function in animals, plants, and microorganisms. *Annu Rev Biochem.* 1987; 56:289–315. An important review summarizing the ferritin’s molecular and cellular biological informations. [PubMed: 3304136]
18. Jain SK, Barrett KJ, Boyd D, et al. Ferritin H and L chains are derived from different multigene families. *J Biol Chem.* 1985; 260:11762–68. [PubMed: 3840163]
19. Torti SV, Kwak EL, Miller SC, et al. The molecular cloning and characterization of murine ferritin heavy chain, a tumor necrosis factor-inducible gene. *J Biol Chem.* 1988; 263:12638–44. [PubMed: 3410854]
20. Pan YH, Sader K, Powerll JJ, et al. 3D morphology of the human hepatic ferritin mineral core: new evidence for a subunit structure revealed by single particle analysis of HAADF-STEM images. *J Struct Biol.* 2009; 166:22–31. [PubMed: 19116170]
21. Ensign D, Young M, Douglas T. Photocatalytic synthesis of copper colloids from CuII by the ferrihydrite core of ferritin. *Inorg Chem.* 2004; 43:3441–6. [PubMed: 15154806]

22. Hosein HA, Strongin DR, Allen M, Douglas T. Iron and cobalt oxide and metallic nanoparticles prepared from ferritin. *Langmuir*. 2004; 20:10283–7. [PubMed: 15518526]
23. Sanchez P, Valero E, Galvez N, et al. MRI relaxation properties of water-soluble apoferritin-encapsulated gadolinium oxide-hydroxide nanoparticles. *Dalton Trans*. 2009:800–4. [PubMed: 19156273]
24. Okuda M, Suzumoto Y, Yamashita I. Bioinspired synthesis of homogenous cerium oxide nanoparticles and two- or three-dimensional nanoparticle arrays using protein supramolecules. *Cryst Growth Des*. 2011; 11:2540–5.
25. Takahashi T, Kuyucak S. Functional properties of threefold and fourfold channels in ferritin deduced from electrostatic calculations. *Biophys J*. 2003; 84:2256–63. [PubMed: 12668434]
26. Yang DW, Nagayama K. Permeation of small molecules into the cavity of ferritin as revealed by proton nuclear-magnetic-resonance relaxation. *Biochem J*. 1995; 307:253–6. [PubMed: 7717984]
27. Stefanini S, Cavallo S, Wang CQ, et al. Thermal stability of horse spleen apoferritin and human recombinant H apoferritin. *Arch Biochem Biophys*. 1996; 325:58–64. [PubMed: 8554343]
- 28•. Kim M, Rho Y, Jin KS, et al. pH-dependent structures of ferritin and apoferritin in solution: disassembly and reassembly. *Biomacromolecules*. 2011; 12:1629–40. An important paper describing the process of ferritin cage disassembly and reassembly mediated by pH shift. [PubMed: 21446722]
- 29•. Aime S, Frullano L, Crich SG. Compartmentalization of a gadolinium complex in the apoferritin cavity: A route to obtain high relaxivity contrast agents for magnetic resonance imaging. *Angew Chem Int Ed*. 2002; 114:1059–61. An excellent paper describing gadolinium complex was encapsulated into ferritin cage via disassociation of cage.
30. Yan F, Zhang Y, Yuan H, et al. Apoferritin protein cages: a novel drug nanocarrier for photodynamic therapy. *Chem Commun*. 2008:4579–81.
31. Yang Z, Wang X, Diao H, et al. Encapsulation of platinum anticancer drugs by apoferritin. *Chem Commun (Camb)*. 2007:3453–5. [PubMed: 17700879]
32. Ruoslahti E. RGD and other recognition sequences for integrins. *Annu Rev Cell Dev Biol*. 1996; 12:697–715. [PubMed: 8970741]
33. Marchesi VT, Tillack TW, Jackson RL, et al. Chemical characterization and surface orientation of the major glycoprotein of the human erythrocyte membrane. *Proc Natl Acad Sci US A*. 1972; 69:1445–9.
34. Uchida M, Flenniken ML, Allen M, et al. Targeting of cancer cells with ferrimagnetic ferritin cage nanoparticles. *J Am Chem Soc*. 2006; 128:16626–33. [PubMed: 17177411]
35. Bartzokis G, Tishler TA. MRI evaluation of basal ganglia ferritin iron and neurotoxicity in Alzheimer's and Huntington's disease. *Cell Mol Biol (Noisy-le-grand)*. 2000; 46:821–33. [PubMed: 10875443]
36. Danon D, Skutelsk E, Marikovs Y, Goldstei L. Use of cationized ferritin as a label of negative charges on cell surfaces. *J Ultrastruct Res*. 1972; 38:500–10. [PubMed: 4111070]
37. Deen WM, Lazzara MJ, Myers BD. Structural determinants of glomerular permeability. *Am J Physiol Renal Physiol*. 2001; 281:F579–96. [PubMed: 11553505]
38. Bennett KM, Bertram JF, Beeman SC, Gretz N. The emerging role of MRI in quantitative renal glomerular morphology. *Am J Physiol Renal Physiol*. 2013; 304:F1252–7. [PubMed: 23515719]
39. Bennett KM, Zhou H, Sumner JP, et al. MRI of the basement membrane using charged nanoparticles as contrast agents. *Magn Reson Med*. 2008; 60:564–74. [PubMed: 18727041]
40. Beeman SC, Zhang M, Gubhaju L, et al. Measuring glomerular number and size in perfused kidneys using MRI. *Am J Physiol Renal Physiol*. 2011; 300:F1454–7. [PubMed: 21411479]
41. Gossuin Y, Muller RN, Gillis P, Bartel L. Relaxivities of human liver and spleen ferritin. *Magn Reson Imaging*. 2005; 23:1001–4. [PubMed: 16376184]
42. Campan M, Lionetti V, Aquaro GD, et al. Ferritin as a reporter gene for in vivo tracking of stem cells by 1-T cardiac MRI in a rat model of myocardial infarction. *Am J Physiol Heart Circ Physiol*. 2011; 300:H2238–50. [PubMed: 21335465]
43. Cohen B, Dafni H, Meir G, et al. Ferritin as an endogenous MRI reporter for noninvasive imaging of gene expression in C6 glioma tumors. *Neoplasia*. 2005; 7:109–17. [PubMed: 15802016]

44. Cohen B, Ziv K, Plaks V, et al. MRI detection of transcriptional regulation of gene expression in transgenic mice. *Nat Med.* 2007; 13:498–503. [PubMed: 17351627]
45. Cao C, Wang X, Cai Y, et al. Targeted in vivo imaging of microscopic tumors with ferritin-based nanoprobes across biological barriers. *Adv Mater.* 2014; doi: 10.1002/adma.201304544
46. Gossuin Y, Muller RN, Gillis P. Relaxation induced by ferritin: a better understanding for an improved MRI iron quantification. *NMR Biomed.* 2004; 17:427–32. [PubMed: 15526352]
47. Li L, Fang CJ, Ryan JC, et al. Binding and uptake of H-ferritin are mediated by human transferrin receptor-1. *Proc Natl Acad Sci US A.* 2010; 107:3505–10.
48. Kalman FK, Geninatti-Crich S, Aime S. Reduction/dissolution of a beta-MnOOH nanophase in the ferritin cavity to yield a highly sensitive, biologically compatible magnetic resonance imaging agent. *Angew Chem Int Ed Engl.* 2010; 49:612–5. [PubMed: 20013829]
49. Geninatti Crich S, Bussolati B, Tei L, et al. Magnetic resonance visualization of tumor angiogenesis by targeting neural cell adhesion molecules with the highly sensitive gadolinium-loaded apoferritin probe. *Cancer Res.* 2006; 66:9196–201. [PubMed: 16982763]
50. Bremer C, Tung CH, Weissleder R. In vivo molecular target assessment of matrix metalloproteinase inhibition. *Nat Med.* 2001; 7:743–8. [PubMed: 11385514]
51. Lee S, Cha EJ, Park K, et al. A near-infrared-fluorescence-quenched gold-nanoparticle imaging probe for in vivo drug screening and protease activity determination. *Angew Chem Int Ed Engl.* 2008; 47:2804–7. [PubMed: 18306196]
52. Butts CA, Swift J, Kang SG, et al. Directing noble metal ion chemistry within a designed ferritin protein. *Biochemistry.* 2008; 47:12729–39. [PubMed: 18991401]
53. Ueno T, Abe M, Hirata K, et al. Process of accumulation of metal ions on the interior surface of apo-ferritin: crystal structures of a series of apo-ferritins containing variable quantities of Pd(II) ions. *J Am Chem Soc.* 2009; 131:5094–100. [PubMed: 19317403]
54. Murray-Kolb LE, Welch R, Theil EC, Beard JL. Women with low iron stores absorb iron from soybeans. *Am J Clin Nutr.* 2003; 77:180–4. [PubMed: 12499339]
55. Sayers MH, Lynch SR, Jacobs P, et al. The effects of ascorbic acid supplementation on the absorption of iron in maize, wheat and soya. *Br J Haematol.* 1973; 24:209–18. [PubMed: 4736579]
56. Powell JJ, Bruggraber SF, Faria N, et al. A nano-disperse ferritin-core mimetic that efficiently corrects anemia without luminal iron redox activity. *Nanomedicine.* 2014; doi: 10.1016/j.nano.2013.12.011
57. MaHam A, Tang ZW, Wu H, et al. Protein-based nanomedicine platforms for drug delivery. *Small.* 2009; 5:1706–21. An important review summarizing the properties of various protein-based nanomedicine platforms for drug delivery. [PubMed: 19572330]
58. Fisher J, Devraj K, Ingram J, et al. Ferritin: a novel mechanism for delivery of iron to the Brain and other organs. *Am J Physiol Cell Physiol.* 2007; 293:C641–9. [PubMed: 17459943]
59. Moss D, Fargion S, Fracanzani AL, et al. Functional roles of the ferritin receptors of Human liver, hepatoma, lymphoid and erythroid cells. *J Inorg Biochem.* 1992; 47:219–27. [PubMed: 1331322]
60. Daniels TR, Delgado T, Rodriguez JA, et al. The transferrin receptor part I: biology and targeting with cytotoxic antibodies for the treatment of cancer. *Clin Immunol.* 2006; 121:144–58. [PubMed: 16904380]
61. Fan K, Cao C, Pan Y, et al. Magnetoferritin nanoparticles for targeting and visualizing Tumour tissues. *Nat Nanotechnol.* 2012; 7:459–64. [PubMed: 22706697]
62. Todd TJ, Zhen Z, Xie J. Ferritin nanocages: great potential as clinically translatable drug delivery vehicles? *Nanomedicine (Lond).* 2013; 8:1555–7. [PubMed: 24074382]
63. Caravan P, Ellison JJ, McMurry TJ, Lauffer RB. Gadolinium(III) chelates as MRI contrast agents: structure, dynamics, and applications. *Chem Rev.* 1999; 99:2293–352. [PubMed: 11749483]

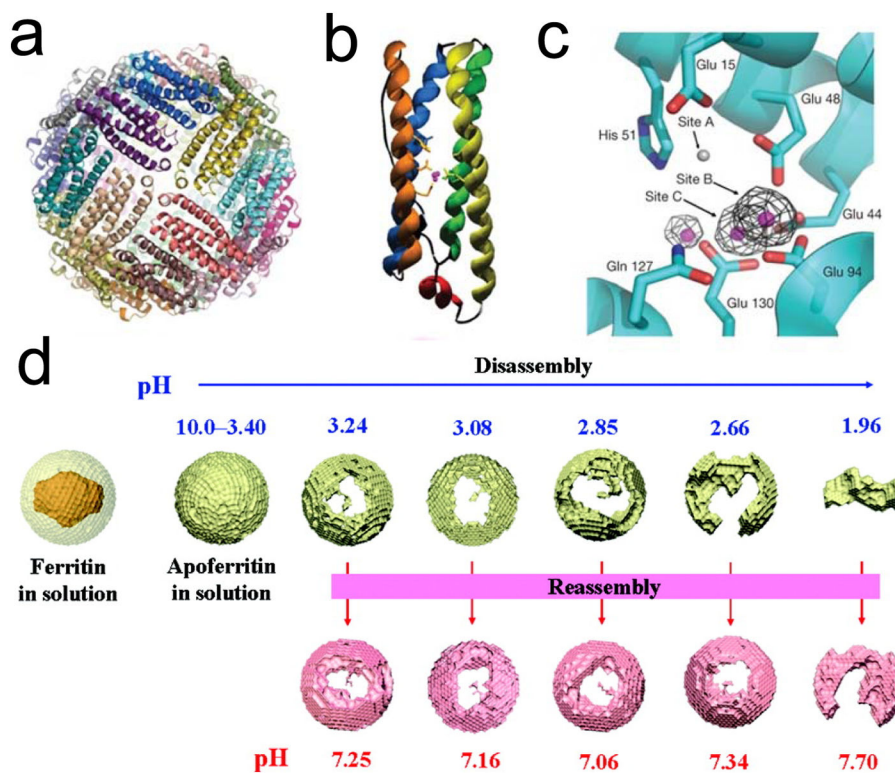


Figure 1. Crystal structure of ferritin and its pH-shift-mediated disassembly and reassembly
a, Crystal structure of recombinant *P. multiseriis* ferritins (24-mer). **b**, Structure of a ferritin monomer. **c**, Ferroxidase site located at ferritin H-chain [16]. **d**, Schematic illustration of pH-mediated disassembly and reassembly of ferritins. Reprinted with permission from ref [28].

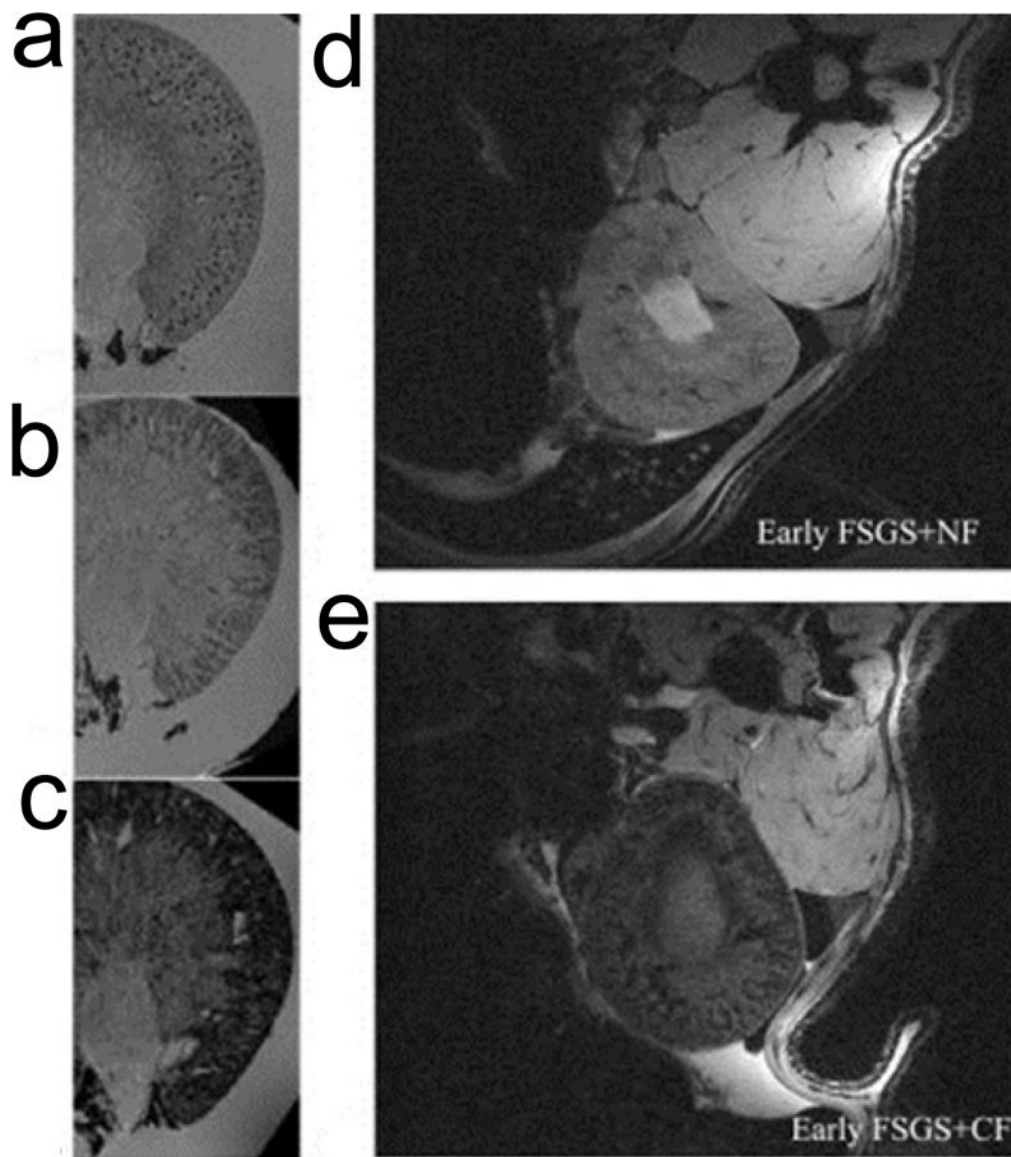


Figure 2. Detection of glomerular injury in puromycin-induced focal and segmental glomerulosclerosis (FSGS) by MRI with cationized ferritins (CF)

a, Ex vivo MRI on normal kidneys, CF was injected beforehand. Spotted distribution of glomeruli was observed. **b**, Ex vivo MRI on kidneys from early FSGS, which was induced by injection of puromycin amnionucleoside (PAN). The spots were still visible but were surrounded by areas of signal hypointensity. **c**, The spots were no longer visible for late FSGS due to enlarged areas of hypointensities. **d**, In vivo MRI of early FSGS after injection of native ferritins (NF). **e**, In vivo MRI of early FSGS after injection of CF. Reprinted with permission from ref [39].

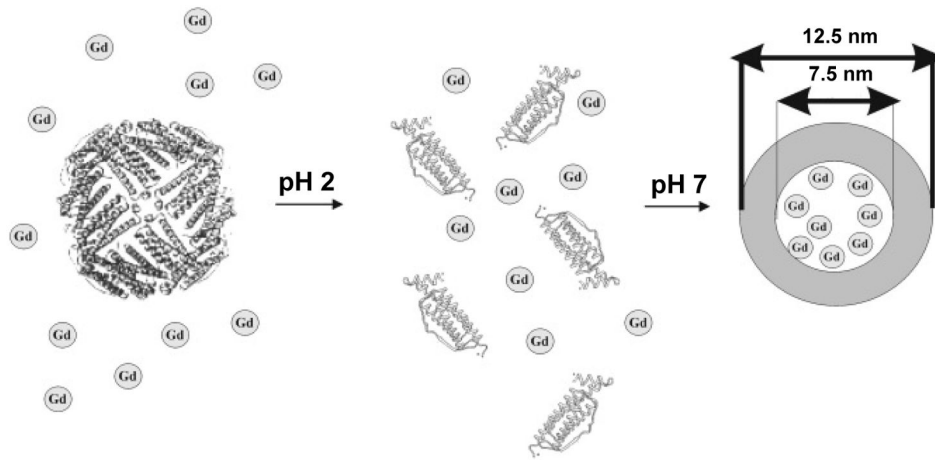


Figure 3. Schematic illustration of loading Gd-HPDO3A into the interiors of ferritins

The nanocages were first disassembled by lowering the pH to 2. Gd-HPDO3A (designated as Gd in the figure) was added to the solution at the low pH. When the pH was tuned back to neutral, the nanocages were reconstituted and Gd-HPDO3A was encapsulated. Reprinted with permission from ref [29].

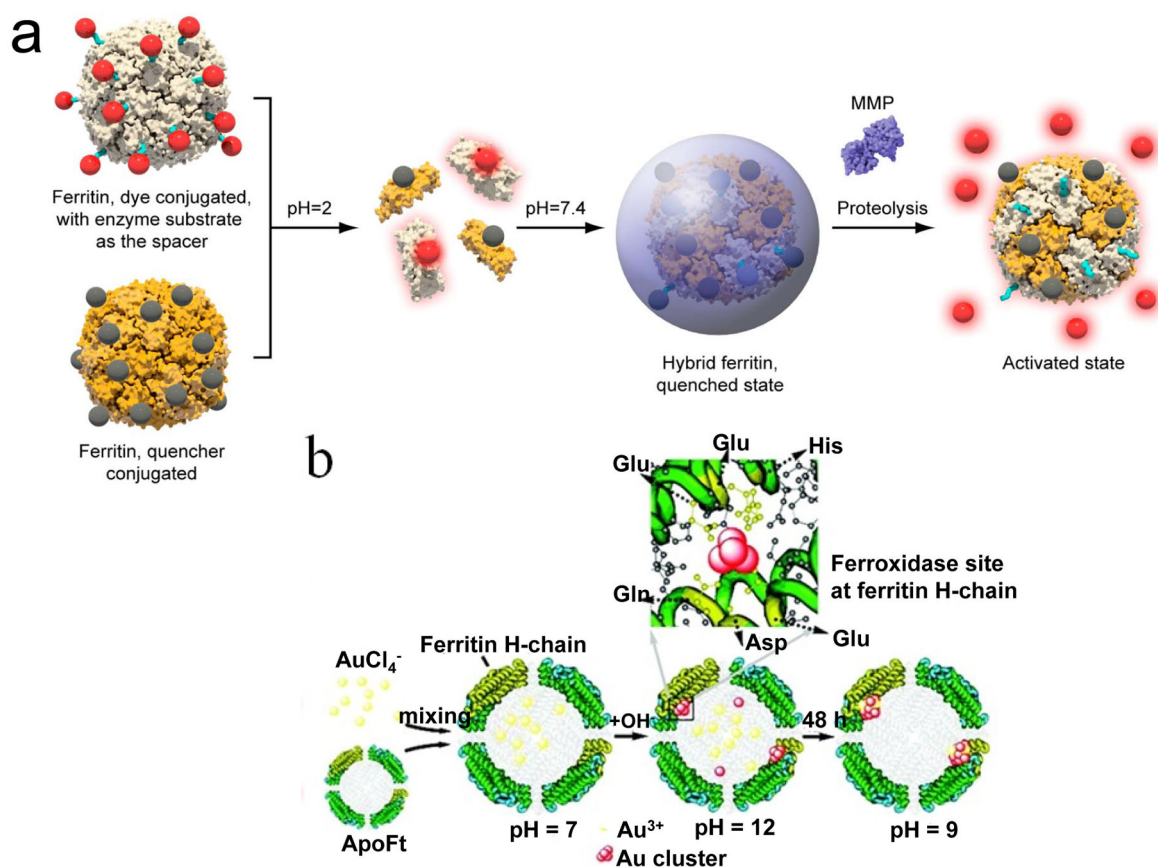


Figure 4. Ferritin-based probes for optical imaging

a, Formation of a ferritin-based MMP activatable probe. *Cy5.5-Gly-Pro-Leu-Gly-Val-Arg-Gly* and black hole quencher-3 (BHQ-3), separately, were conjugated onto two sets of ferritin nanocages. By mixing the two types of ferritin conjugates and subjecting them to pH-mediated hybridization, ferritin nanoparticles presenting both *Cy5.5-GPLGVRG* and BHQ-3 on the surface were yielded. Fluorescence can be activated by proteolysis of MMPs that are highly expressed in tumor masses. Reprinted with permission from ref [10]. **b**, Schematic illustration of the synthesis of Au nanoclusters using ferritins as templates. The His residues at the ferroxidase site played an important role in the in situ Au cluster formation. Reprinted with permission from ref [11].

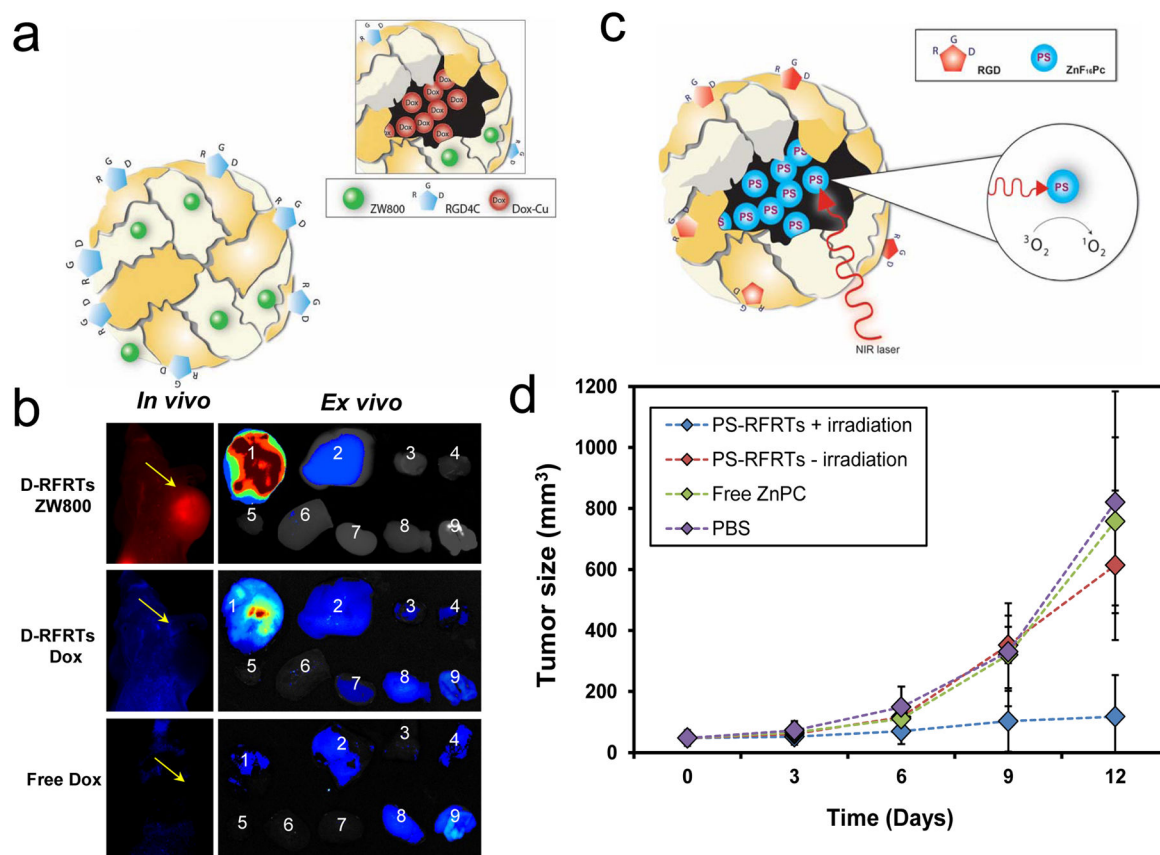


Figure 5. RGD modified ferritins as carriers for therapeutics and photosensitizers

a, Schematic illustration of doxorubicin-loaded, RGD-modified ferritins (D-RFRTs). Doxorubicin (Dox) was pre-complexed with Cu, and the complexes were encapsulated efficiently into RFRTs. **b**, *In vivo* and *ex vivo* imaging results of U87MG tumor-bearing mice injected with ZW800-labeled D-RFRTs and free Dox. For *ex vivo* studies, the organs were arranged in the following order: 1, tumor; 2, liver; 3, lung; 4, muscle; 5, heart; 6, spleen; 7, kidneys; 8, brain; 9, intestine. With ferritins as carriers, significantly enhanced tumor uptake of Dox was achieved. Reprinted with permission from ref [12]. **c**, Formation and working mechanism of ZnF₁₆Pc-loaded, RGD-modified ferritins (P-RFRTs). ZnF₁₆Pc can be loaded into RFRTs with high efficiency. Under irradiation of a 671 nm laser, ZnF₁₆Pc can transfer energy to near-by O₂ molecules to yield ¹O₂. **d**, Tumor growth can be suppressed by P-RFRTs-mediated photodynamic therapy (PDT). U87MG tumor bearing mice were divided into four groups which received different treatments. Group 1: P-RFRTs, with irradiation. Group 2: P-RFRTs, without irradiation. Group 3: ZnF₁₆Pc, with irradiation. Group 4: PBS, without irradiation. Significant tumor suppression was found in group 1 ($P < 0.05$). On day 12, a tumor inhibition rate (TIR) of $83.64 \pm 2.52\%$ was observed. Reprinted with permission from ref [9].